ISSN 1674-1056
http://cpb.iphy.ac.cn
http://iopscience.iop.org/cpb
中国物理 B
Chinese Physics
中国物理
Chinese Physics B

New design of ferroelectric solar cell combined with luminescent solar concentrator

Slimane Latreche, Mohamed Fathi, Abderrahmane Kadri

Citation: Chin. Phys. B . 2019, 28(8): 088801. **doi:** 10.1088/1674-1056/28/8/088801
Journal homepage: http://cpb.iphy.ac.cn; http://iopscience.iop.org/cpb

What follows is a list of articles you may be interested in

Effect of defects properties on InP-based high electron mobility transistors

Shu-Xiang Sun(孙树祥), Ming-Ming Chang(常明铭), Meng-Ke Li(李梦珂), Liu-Hong Ma(马刘红), Ying-Hui Zhong(钟英辉), Yu-Xiao Li(李玉晓), Peng Ding(丁芃), Zhi Jin(金智), Zhi-Chao Wei(魏志超)
Chin. Phys. B . 2019, 28(7): 078501. **doi:** 10.1088/1674-1056/28/7/078501

Dark count rate and band to band tunneling optimization for single photon avalanche diode topologies

Taha Haddadifam, Mohammad Azim Karami
Chin. Phys. B . 2019, 28(6): 068502. **doi:** 10.1088/1674-1056/28/6/068502

Modeling electric field of power metal-oxide-semiconductor field-effect transistor with dielectric trench based on Schwarz-Christoffel transformation

Zhi-Gang Wang(汪志刚), Tao Liao(廖涛), Ya-Nan Wang(王亚南)
Chin. Phys. B . 2019, 28(5): 058503. **doi:** 10.1088/1674-1056/28/5/058503

Optimization of ambipolar current and analog/RF performance for T-shaped tunnel field-effect transistor with gate dielectric spacer

Ru Han(韩茹), Hai-Chao Zhang(张海潮), Dang-Hui Wang(王党辉), Cui Li(李翠)
Chin. Phys. B . 2019, 28(1): 018505. **doi:** 10.1088/1674-1056/28/1/018505

Analysis of tail bits generation of multilevel storage in resistive switching memory

Jing Liu(刘璟), Xiaoxin Xu(许晓欣), Chuanbing Chen(陈传兵), Tiancheng Gong(龚天成), Zhaoan Yu(余兆安), Qing Luo(罗庆), Peng Yuan(袁鹏), Danian Dong(董大年), Qi Liu(刘琦), Shibing Long(龙世兵), Hangbing Lv(吕杭炳), Ming Liu(刘明)
Chin. Phys. B . 2018, 27(11): 118501. **doi:** 10.1088/1674-1056/27/11/118501

New design of ferroelectric solar cell combined with luminescent solar concentrator

Slimane Latreche[1,2,†], Mohamed Fathi[1], and Abderrahmane Kadri[2]

[1] *Unité de Développement des Equipements Solaires, UDES/Centre de Développement des Energies Renouvelables, CDER, Tipaza* 42415, *Algeria*

[2] *Laboratoire d'Etude des Matériaux Optoélectronique & Polymères, Department of Physics, University of Oran* 1 *Ahmed Ben Bella, BP* 1524 *El M'Naouer, Oran* 31000, *Algeria*

(Received 11 March 2019; revised manuscript received 20 May 2019; published online 9 July 2019)

A new transparent photovoltaic panel composed of a luminescent solar concentrator and Al/$BaTiO_3$/ZnO/Pt ferroelectric solar cells is presented, in which a portion of the incoming solar illumination is converted by the fluorophores to ultraviolet (UV) light which is then absorbed by ZnO. Firstly, the solar cells are simulated using Atlas–Silvaco. Then, the panel is modelled based on the obtained solar cell characteristics. This panel would be of great importance for building integrated photovoltaics domain because of its high transparency.

Keywords: Atlas–Silvaco, ferroelectric solar cell, luminescent solar concentrator, building integrated photovoltaic

PACS: 88.40.J–, 85.30.De, 88.40.H–, 88.40.mr **DOI:** 10.1088/1674-1056/28/8/088801

1. Introduction

Photovoltaic solar energy is the object of many scientific investigations. Researchers are constantly looking for cleaner, more efficient, and less costly systems. The pn junction solar cell (PNJSC) is the most used cell for solar energy harvesting,[1–3] and it is generally fabricated with silicon[1] containing a junction between two differently doped regions p and n; as a result, a build-in electric field appears therein, which separates the photogenerated charge carriers,[3–5] so the electrons and holes are drifted to the n and p regions, respectively, and then collected by the poles. Lastly, electrons will flow in the external circuit to provide energy and recombine with holes.[4,5]

Although PNJSCs are the most commercialized solar cells, many obstacles therein have to be surmounted in order to increase their efficiency again.[3–6] Among the solar light photons, only those with energy equal or higher than the semiconductor band gap energy (E_g) will be exploited; in addition, the excess energy coming from photons with the energy higher than E_g will raise the crystal temperature because of the photogenerated electrons and holes thermalization, which means that the output energy of the cell will be decreased.[4,5,7–9] In addition, the open circuit voltage (V_{oc}) of a PNJSC is less than E_g/e (e is the elementary charge value)[3–5,10] and the attempt of increasing this voltage by adding dopants favors the non-radiative recombination; hence, the yield is reduced.[5]

Heterojunction solar cells are developed with the aim of absorbing the solar illumination more efficiently,[4–6,11] and their theoretical efficiency limit for an infinite number of junctions may reach 69%, 86%–86.8% under one sun, full concentration, respectively.[4,11,12] However, this type of cells is limited in material choice and has a high cost since it requires advanced growth techniques.[6]

Ferroelectric materials (FMs) under a specific temperature (Curie temperature) are characterised by an electric field which presents a hysteresis cycle, so it can be controlled by applying an electric field.[13] Since FMs present photovoltaic effect, many researchers have developed new solar cell structures based on these materials.[2,3,10,14–18]

At the beginning of ferroelectric solar cells (FSCs), the FM was used as a light absorber wherein the ferroelectric electric field is responsible for charge carrier separation. These cells present high values of V_{oc} originated from the domain walls,[2,18] however, their short circuit current I_{sc} is very low due to the weak electrical conductivity and the high E_g, which means that a small amount of charge carriers are generated using solar spectrum.[14,17,19]

In order to avoid these problems, FMs have been combined with a semiconductor light absorber. Fang Huang and Xiangxin Liu[15] fabricated a photovoltaic device in which the active layer is composed of CdTe absorber and CdS ferroelectric nanoparticles. Since the interface between CdS nanoparticles and CdTe is very important, the output current of this device is reduced due to surface recombination.[5]

A new approach to exploit FMs in photovoltaic cells was proposed by Wang *et al.*[19] in which FM was used to apply an

†Corresponding author. E-mail: slimane.latreche@gmail.com

© 2019 Chinese Physical Society and IOP Publishing Ltd

electric field on a semiconductor absorber layer and, hence, to separate photogenerated carriers. In this new cell, photocurrent does not pass through the FM and photogeneration occurs at the semiconductor layer, which means that important I_{sc} is accessible; nevertheless, the non-uniformity of the electric field and its weakness compared to the PNJSC limit the cell efficiency.

Luminescent solar concentrators (LSCs) have been studied for many reasons, such as their building compatibility and their economy since fewer solar cells are needed.[20–25] Down/up-conversion is a process in which particles absorb photons and then emit light at longer/shorter wavelength than the excitation wavelength. Many researchers are interested in down-conversion fluorophores embedded in LSCs[7,8,20,23,26–28] because silicon solar cells are the most used; however, up-conversion is also studied in order to benefit from longer wavelength radiations.[8,9,28]

In this theoretical work, we introduce a new transparent photovoltaic panel that is composed of ferroelectric solar cells and a luminescent solar concentrator, which can be realized using actual fabrication technologies. The panel schematics and its working principle are well explained in Section 2. Using ATLAS-Silvaco, we simulate and calculate the efficiency of Al/$BaTiO_3$/ZnO/Pt ferroelectric solar cells; then, we calculate the transparent panel characteristics.

2. Proposition

Figures 1 and 2 present the front view and cross section of the proposed solar panel, respectively. As shown in Fig. 2, a portion of the solar light is converted to ultraviolet (UV) radiation by the electroluminescent particles embedded in the LSC layer. The remaining part of the solar light is transmitted to the indoor environment. The UV emitted photons are guided to the solar cells' edges where they are absorbed. Since the width of the cells is on the order of a few μm, the position, the orientation, and the spacing between them can be changed in order to maximize the efficiency of the LSC without altering the transparency of the panel, unlike other building-integrated photovoltaics.[25]

This panel structure is also suitable for other types of solar cells, such as silicon cell if the following conditions are met:

(i) The width of the cell must be comparable to the penetration depth.

(ii) The light absorber layer must be aligned with the electroluminescent layer.

(iii) The luminescent particles should be chosen in such a way that the emitted photon energy corresponds to the gap energy of the light absorbing material.

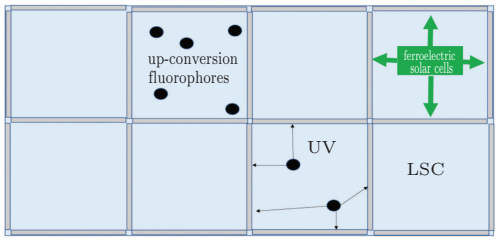


Fig. 1. A front view scheme of the proposed transparent photovoltaic panel.

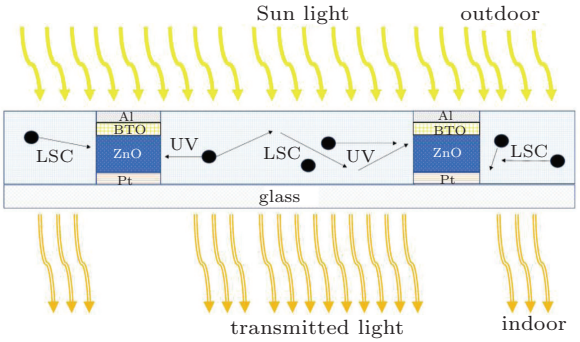


Fig. 2. A cross section scheme of the proposed transparent photovoltaic panel.

3. Luminescent solar concentrator

ZnO is a large band gap (3.4 eV)[29] semiconductor, hence, on the one hand, up-conversion luminescent elements must be embedded in the transparent matrix, with emission wavelengths less than 364 nm. Many up-conversion fluorophores are introduced in the literature. Table 1 resumes some UV emitting fluorophores; on the other hand, UV emitted light reabsorption must be minimized; therefore, the LSC must be with limited UV absorption material, such as glass as an example.[30]

The fluorophores proposed here emit several wavelengths, but, in our case, only the ones less than 364 nm are utile for photogeneration.

Table 1. UV emitting up-conversion fluorophores.

Fluorophore	Absorption/nm	Emission/nm	Ref.
$NaYF_4$:Yb^{3+}, Tb^{3+}	976	350, 370, 417, 455, 476, 526, 540, 645, 667	[8]
LuPO4:Yb^{3+}, Tm^{3+}	978	360, 455, 476, 660, 800	[8]
NaLuF4:Yb, Tm	(IR)	345, 362, 450, 473, 646, 802	[31]

3.1. Ferroelectric solar cell

Using Atlas–Silvaco software, two solar cells are simulated. These cells have vertical generation and lateral collection of the light generated carriers.[32] This type of cells suits the LSC perfectly. We remind that Atlas-Silvaco is a semiconductor device simulator, which is based on Poisson's equation, the continuity equation, and the transport equation for electrons and holes.[33] In all our simulations, we consider the temperature $T = 300$ K and the wavelength of the monochromatic incident illumination $\lambda = 350$ nm with an intensity of 1 W/cm^2 unless other values are mentioned. These values are chosen because the solar cells receive a monochromatic concentrated light in the UV range, which comes from the LSC.

Firstly, we simulate cells composed of n-doped ZnO as an absorber, and Al and Pt as electrodes, as shown in Fig. 3.

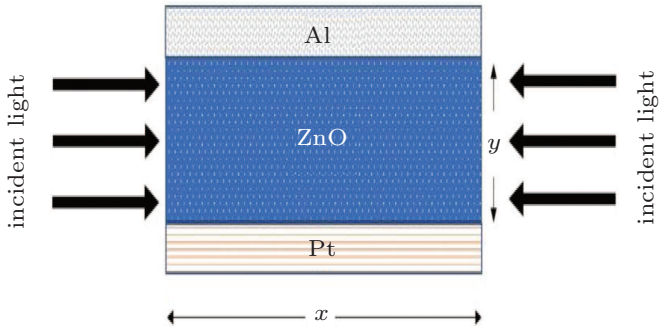


Fig. 3. A Schematic representation of the simulated Al/ZnO/Pt solar cell.

Platinum (Pt) has a work function of 5.7 eV[34] and zinc oxide (ZnO) has an electronic affinity of 2.088 eV,[35] hence, the n-ZnO/Pt forms a Schottky contact in which a spatial charge zone takes place near the junction. Photogenerated carriers in this region are diffused in different senses depending on their charge sign, so the separation is realized.

Secondly, we add a ferroelectric $BaTiO_3$ (BTO) layer to our cell to form an Al/BTO/ZnO/Pt cell which is schematically represented in Fig. 4.

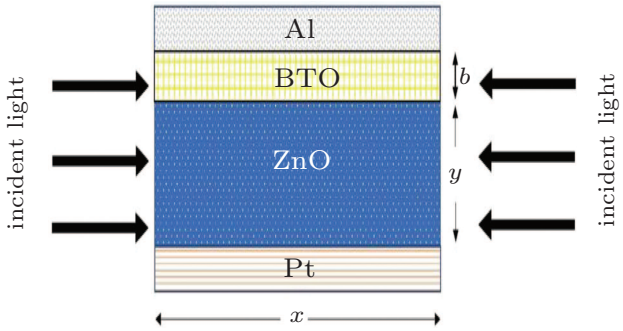


Fig. 4. The Schematic representation of the simulated Al/BTO/ZnO/Pt solar cell.

Several cell dimensions (ZnO and BTO layer thickness, cell width) are compared in order to optimize the efficiency.

4. Results and discussion

4.1. Solar cell simulation results

4.1.1. Solar cell without ferroelectric layer

Al/ZnO/Pt solar cells with different dimensions x and y as shown in Fig. 3 are simulated, and the following figures 5–9 show the current density–voltage (J–V) characteristics. In this work, the dimensions are in the unit of μm unless another unit is mentioned. Also, the current and power densities are calculated with respect to the light collecting face area (edge surface).

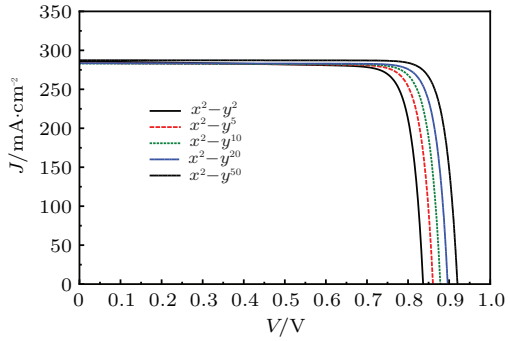


Fig. 5. The J–V characteristics for Al/ZnO/Pt cells with $x = 2$ μm.

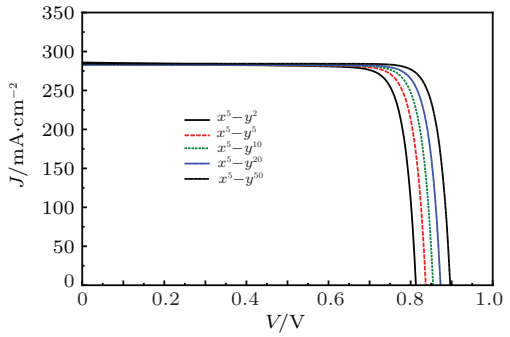


Fig. 6. The J–V characteristics for Al/ZnO/Pt cells with $x = 5$ μm.

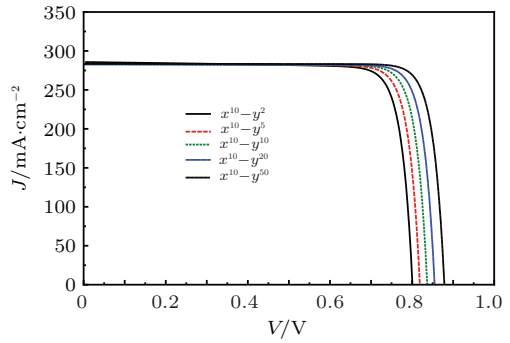


Fig. 7. The J–V characteristics for Al/ZnO/Pt cells with $x = 10$ μm.

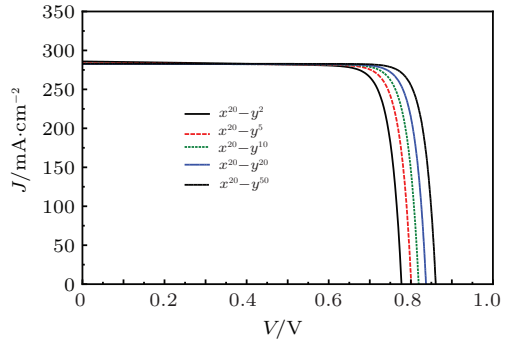


Fig. 8. The J–V characteristics for Al/ZnO/Pt cells with $x = 20$ μm.

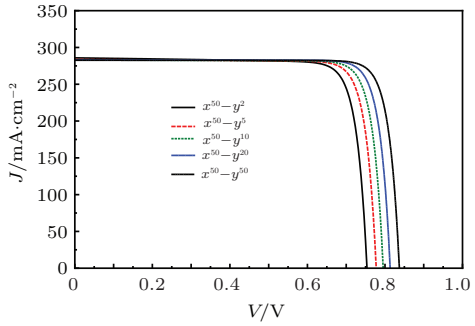


Fig. 9. The *J*–*V* characteristics for Al/ZnO/Pt cells with $x = 5$ μm.

We note that the short circuit current density is practically the same for all the dimensions, however, the open circuit voltage increases with the cell thickness unlike conventional solar cells,[36] and this is because the incidence of light is perpendicular to the cell thickness direction. Also, the voltage drops for a greater width x due to the diffusion of photogenerated carriers from the edges toward the middle. This diffusion occurs because of the photogeneration rate gradient as illustrated in Fig. 10.

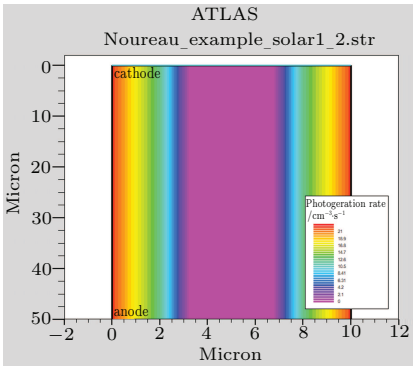


Fig. 10. Photogeneration rates. The photogeneration gradients are oriented from the center toward the edges.

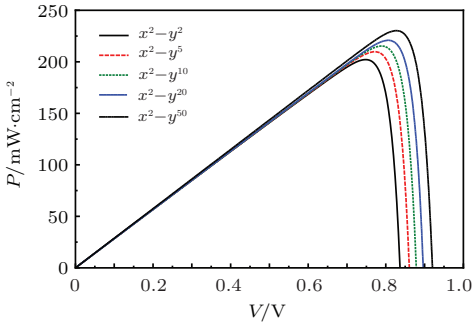


Fig. 11. The *P*–*V* characteristics for Al/ZnO/Pt cells with $x = 2$ μm.

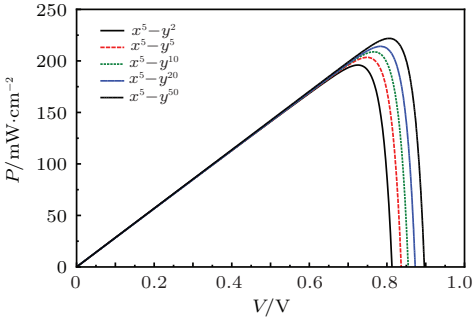


Fig. 12. The *P*–*V* characteristics for Al/ZnO/Pt cells with $x = 5$ μm.

Figures 11–15 show the power density–voltage (*P*–*V*) characteristics; the essential difference is the open circuit voltage, and the maximum power is greater for smaller x and greater y values.

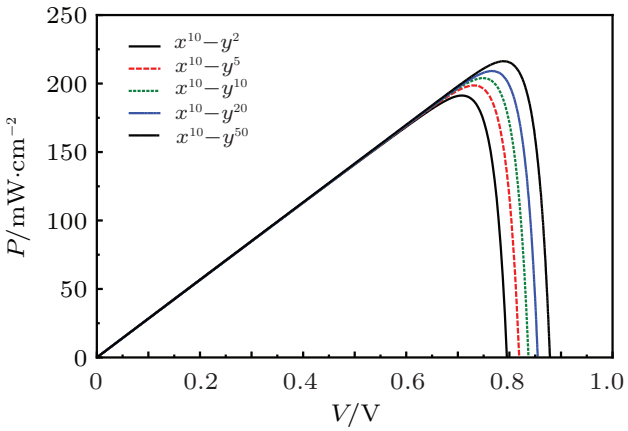


Fig. 13. The *P*–*V* characteristics for Al/ZnO/Pt cells with $x = 10$ μm.

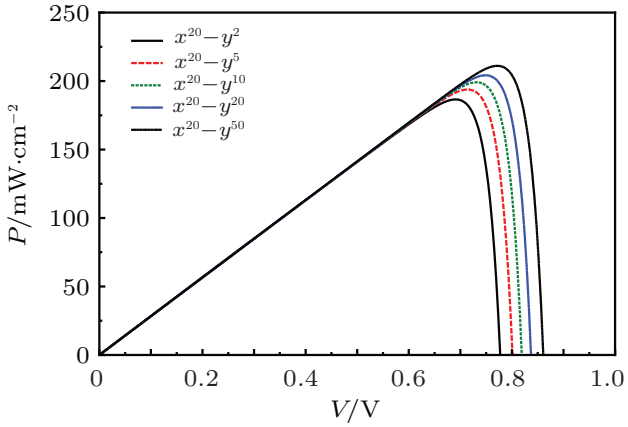


Fig. 14. The *P*–*V* characteristics for Al/ZnO/Pt cells with $x = 20$ μm.

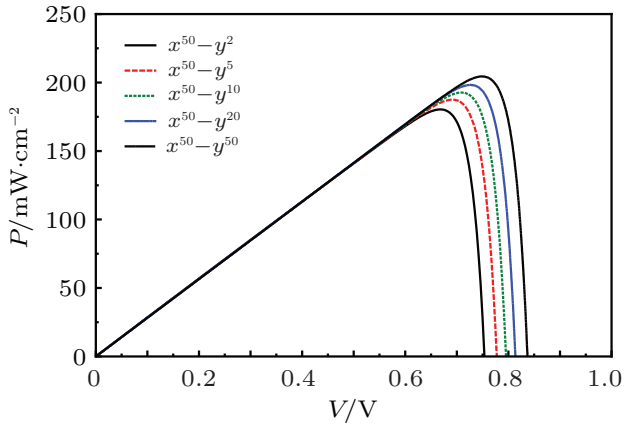


Fig. 15. The *P*–*V* characteristics for Al/ZnO/Pt cells with $x = 50$ μm.

One can see that the short circuit current behavior is not so clear, but generally it increases with the thickness of zinc oxide and decreases slightly with the cell width; however, it is clear that the open circuit voltage varies depending on the cell parameters. Summarily, the power output is greater for $x = 2$ and $y = 50$.

4.1.2. Solar cell with ferroelectric layer

We have simulated a number of Al/BTO/ZnO/Pt solar cells with the width value $x = 2$ and different ZnO and BTO thicknesses y and b, respectively, as shown in Fig. 4. The value of x is chosen based on the previous results, where it was found that decreasing the width of the cell, x gives better results. In Figs. 16–20, we show the current density–voltage characteristics.

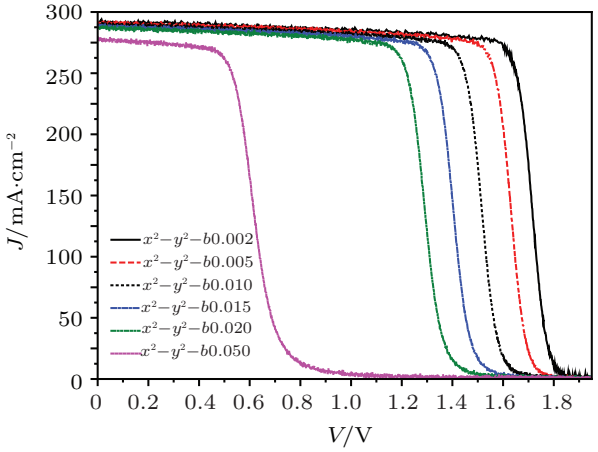


Fig. 16. The J–V characteristics for Al/BTO/ZnO/Pt cells with $x = 2$ μm and $y = 2$ μm.

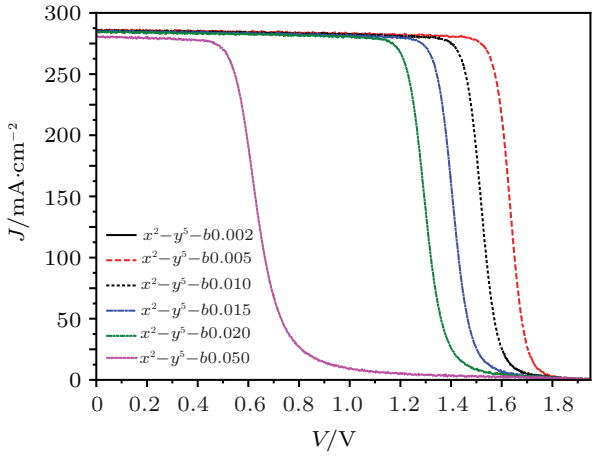


Fig. 17. The J–V characteristics for Al/BTO/ZnO/Pt cells with $x = 2$ μm and $y = 5$ μm.

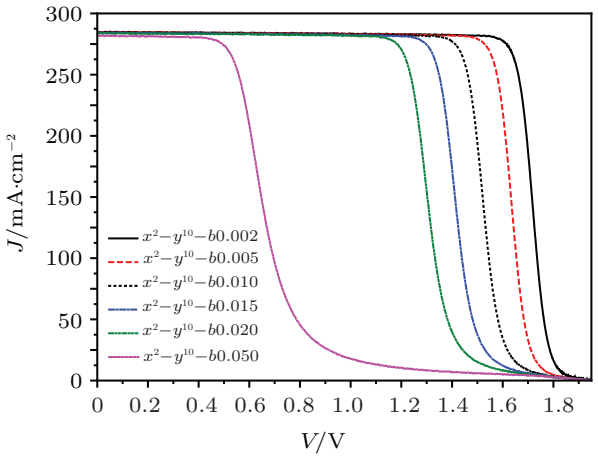


Fig. 18. The J–V characteristics for Al/BTO/ZnO/Pt cells with $x = 2$ μm and $y = 10$ μm.

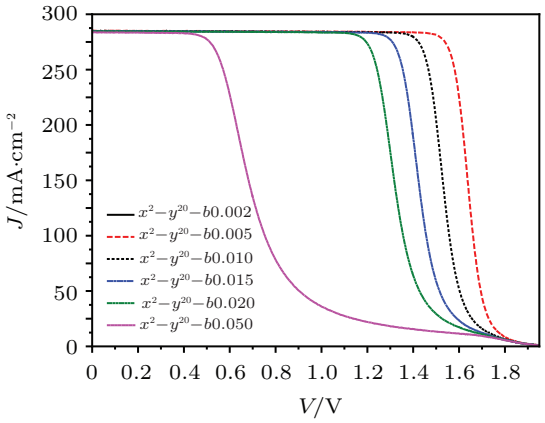


Fig. 19. The J–V characteristics for Al/BTO/ZnO/Pt cells with $x = 2$ μm and $y = 20$ μm.

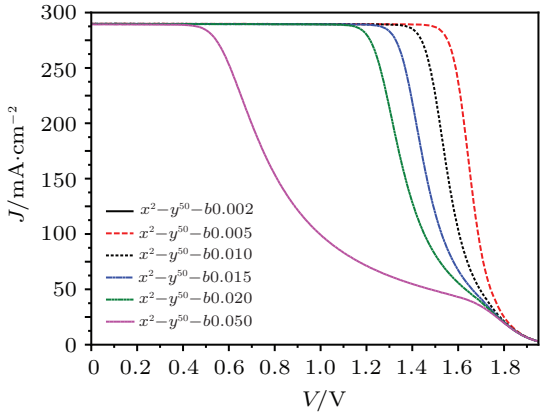


Fig. 20. The J–V characteristics for Al/BTO/ZnO/Pt cells with $x = 2$ μm and $y = 50$ μm.

It is evident from Figs. 16–20 that the short circuit current depends just slightly on ZnO and BTO thicknesses y and b, and the open circuit voltage increases with y. This increase is the result of the ferroelectric polarization. It is clear that the characteristic shape varies drastically as b changes. Lower fill factors are obtained when BTO layer is thicker and this is due to the resistivity of the material.

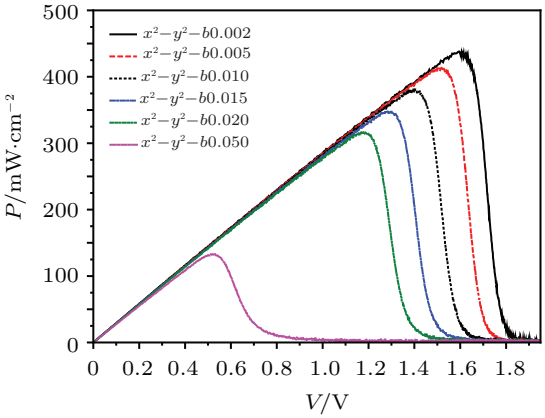


Fig. 21. The P–V characteristics for Al/BTO/ZnO/Pt cells with $x = 2$ μm and $y = 2$ μm.

Figures 21–25 show the power density–voltage characteristics. The open circuit voltage increases for thicker ZnO layers, and the maximum power is greater for thinner BTO

layers. Increasing the latter leads to poorer fill factor. The maximum power output follows the V_{oc} variation and takes its greater value for $y = 50$ and $b = 0.002$.

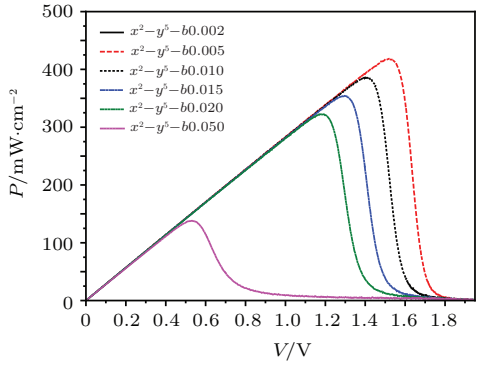


Fig. 22. The *P*–*V* characteristics for Al/BTO/ZnO/Pt cells with $x = 2$ μm and $y = 10$ μm.

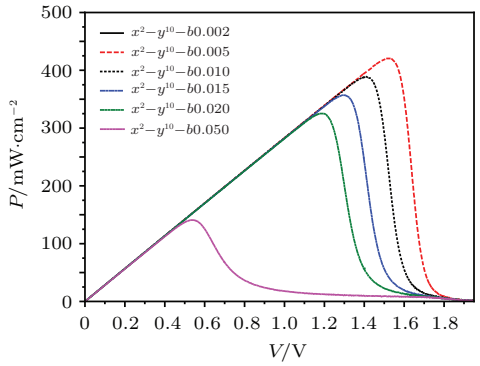


Fig. 23. The *P*–*V* characteristics for Al/BTO/ZnO/Pt cells with $x = 2$ μm and $y = 10$ μm.

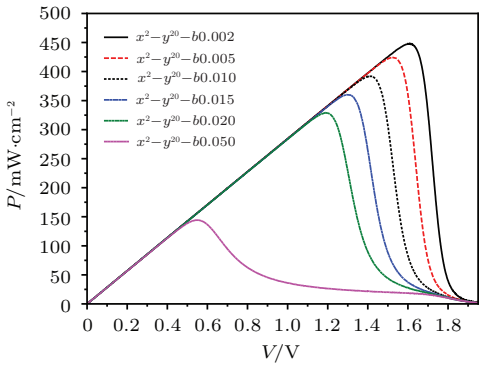


Fig. 24. The *P*–*V* characteristics for Al/BTO/ZnO/Pt cells with $x = 2$ μm and $y = 20$ μm.

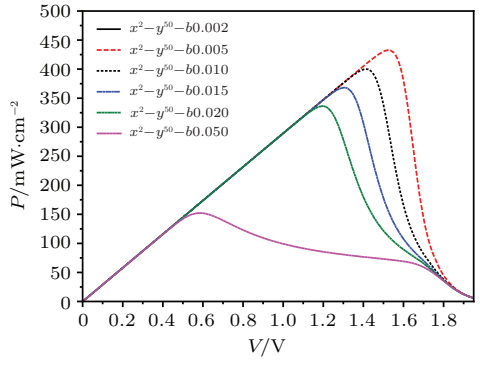


Fig. 25. The *P*–*V* characteristics for Al/BTO/ZnO/Pt cells with $x = 2$ μm and $y = 50$ μm.

4.2. Estimation of the yielding of transparent solar panel

We consider a transparent solar panel as designed in Fig. 2 with a surface of 1 m^2 and 10 ferroelectric cells arranged regularly, one parallel to each other, dividing the panel into 11 small regions as shown in Fig. 26. The cell parameters are chosen ($x = 2$, $y = 50$, $b = 0.002$) based on the results of the solar cell simulation. The panel edges are covered by mirrors to avoid the escape of emitted UV light.

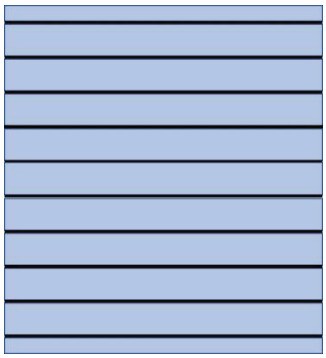


Fig. 26. A schematic diagram of the simulated photovoltaic panel of 1 m^2:$((9 \times 100 \times 10) + (2 \times 100 \times 5))$ cm^2.

Many cell connection methods are possible. In our work, the 10 cells are connected in series. Each cell has a (light collecting) surface

$$S_{\text{cell}} = 100 \times 50.002 \times 10^{-4}\ \text{cm}^2 \approx 0.5\ \text{cm}^2. \tag{1}$$

In this case, the panel efficiency

$$E_{\text{panel}} = E_{\text{LSC}} \times E_{\text{cell}}, \tag{2}$$

where E_{LSC} and E_{cell} are respectively the LSC and the cell's efficiency. E_{LSC} depends on the optical and the quantum efficiencies.

The LSC concentration in our case is the ratio of the incidence surface S_{in} to the emitting edges surface, and the latter is equal to the cell surface S_{cell} multiplied by 2 (because two cells are connected to the LSC), so

$$C_{\text{LSC}} = \frac{S_{\text{in}}}{2 \times S_{\text{cell}}} = \frac{10 \times 100}{2 \times 0.5} = 1000. \tag{3}$$

An incident density J_{in} that contains direct and diffused light is arriving on the top surface of the LSC as shown in Fig. 27. The outcoming UV light with a density J_{out} is collected by cells. The relationship between the two densities is

$$J_{\text{out}} = J_{\text{in}} \times C_{\text{LSC}} \times E_{\text{LSC}}. \tag{4}$$

This is equivalent to

$$\frac{I_{\text{out}}}{S_{\text{cell}}} = \frac{I_{\text{in}}}{S_{\text{in}}} \times \frac{S_{\text{in}}}{2 \times S_{\text{cell}}} \times E_{\text{LSC}}, \tag{5}$$

where I_{out} and I_{in} are respectively the outcoming and the incident light intensities.

By multiplying Eq. (5) by S_{cell}

$$I_{\text{out}} = \frac{I_{\text{in}}}{2} \times E_{\text{LSC}}. \tag{6}$$

The solar cell transforms the outcoming UV light I_{out} into electric energy power P_{cell}; this can be written as

$$P_{\text{cell}} = 2 \times I_{\text{out}} \times E_{\text{cell}}. \tag{7}$$

The factor 2 takes place because the solar cell receives light from two edges.

The solar panel contains 10 cells, so the total power can be written as

$$P_{\text{tot}} = 10 \times P_{\text{cell}}. \tag{8}$$

From Eqs. (6), (7), and (8), we can obtain

$$P_{\text{tot}} = 10 \times I_{\text{in}} \times E_{\text{LSC}} \times E_{\text{cell}}. \tag{9}$$

The cells are connected in series, so the panel I–V characteristic can be deduced from the cell characteristic and the LSC efficiency. The connection resistance is not taken into account.

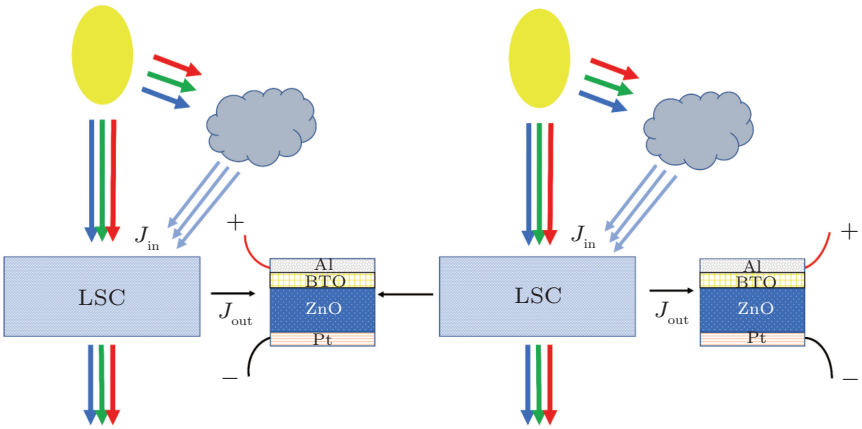


Fig. 27. A simplified schema explaining the energy conversion steps in the system LSC-solar cell.

By considering E_{LSC}=10% and an illumination of 1000 W/m^2, the proposed panel current–voltage (I–V) and power–voltage (P–V) characteristics will be shown in Figs. 28 and 29.

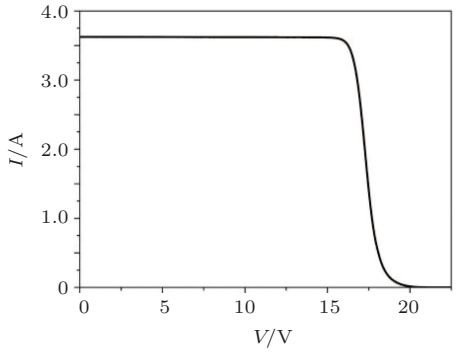


Fig. 28. The I–V characteristics of the transparent solar panel proposed in our work.

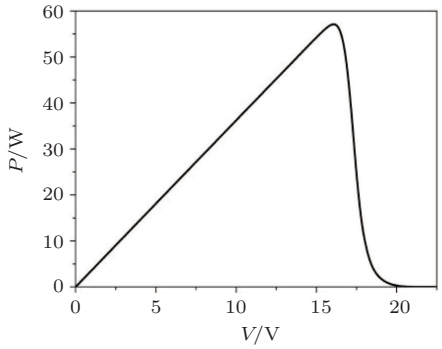


Fig. 29. The P–V characteristics of the transparent solar panel proposed in our work.

The panel characteristics are $V_{\text{oc}} \approx 20$ V, $I_{\text{sc}} = 3.625$ A, $P_{\text{max}} = 57$ W, fill factor=78.7%, $I_{\text{pmax}} = 3.55$ A, and $V_{\text{pmax}} = 16.06$ V. I_{pmax} and V_{pmax} are the maximum power point current and voltage, respectively.

5. Conclusion

In this work, it is shown that luminescent solar concentrator and ferroelectric solar cells can be combined together in order to form a new transparent photovoltaic panel. The ferroelectric solar cells are designed in such a way that the light incidence is lateral, which makes them adapted to luminescent solar concentrator.

Firstly, we commence the simulation using Atlas-Silvaco by considering a Schottky junction solar cell Al/ZnO/Pt. The results show that increasing the ZnO thickness and reducing the cell width lead to better efficiency values. The best simulated cell characteristics are $J_{\text{sc}} = 287.30$ mA/cm^2, $V_{\text{oc}} = 0.92$ V, $P_{\text{max}} = 230.21$ mW/cm^2, fill factor = 0.87, and the efficiency is 11.51%.

Secondly, we simulate the structure Al/BTO/ZnO/Pt to investigate the effect of barium titanate layer on the cell efficiency. It is shown that thinner BTO layers give rise to better efficiency values; however, thicker ones reduce the fill factor, and this occurs due to the material's electrical resistivity. The simulation of an optimized ferroelectric cell gives us

$J_{sc} = 290.00$ mA/cm^2, $V_{oc} = 2.00$ V, $P_{max} = 456.79$ mW/cm^2, fill factor = 0.78, and the efficiency = 22.84%.

Finally, a transparent photovoltaic panel is designed in which LSC absorbs a portion of the incident solar light and converts it to UV light which is guided into the ferroelectric solar cells. By considering the LSC efficiency as 10%, the estimated characteristics of a 1-m^2 panel are $V_{oc} \approx 20$ V, $I_{sc} = 3.62$ A, $P_{max} = 57$ W, $I_{pmax} = 3.55$ A, $V_{pmax} = 16.06$ V, and fill factor = 78.7%. This solar panel is of great interest for the building-integrated photovoltaics (BIPV) domain because of its transparency and the LSC ability to collect the direct and the diffused light simultaneously, leading to important electrical energy generation. The fluorophores types, concentration, and the solar cell materials can be chosen according to the local illumination and the desired transparency-electrical efficiency ratio.

References

[1] Kaushika N D, Mishra A and Rai A K 2018 *Solar Photovoltaics: Technology, System Design, Reliability and Viability* (Cham: Springer International Publishing) p. 10

[2] Ji W, Yao K and Liang Y C 2010 *Adv. Mater.* **22** 1763

[3] Liu F, Wang W, Wang L and Yang G 2014 *Appl. Phys. Lett.* **104** 103907

[4] Nelson J 2003 *The Physics of Solar Cells* (London: Imperial College Press) pp. 02, 88

[5] Würfel P and Würfel U 2016 *Physics of Solar Cells: From Basic Principles to Advanced Concepts* (Weinheim: Wiley-VCH) pp. 65, 82, 111–113, 173, 189

[6] Todorov T K, Bishop D M and Lee Y S 2018 *Sol. Energy Mater. Sol. Cells* **180** 350

[7] Liu N, Li S X, Ye Y C and Yao Y L 2018 *Chin. Phys. B* **27** 127303

[8] Strümpel C, McCann M, Beaucarne G, Arkhipov V, Slaoui A, Švrček V, del Cañizo C and Tobias I 2007 *Sol. Energy Mater. Sol. Cells* **91** 238

[9] Fischer S, Ivaturi A, Jakob P, Krämer K W, Martin-Rodriguez R, Meijerink A, Richards B and Goldschmidt J C 2018 *Opt. Mater.* **84** 389

[10] Qin M, Yao K and Liang Y C 2010 2010 *IEEE International Conference on Sustainable Energy Technologies* (ICSET), December 6–9, 2010, Kandy, Sri Lanka pp. 1–5

[11] Pérez-Higueras P and Fernández E F 2015 *High Concentrator Photovoltaics: Fundamentals, Engineering and Power Plants* (Cham: Springer International Publishing) pp. 9–37

[12] Algora C and Rey-Stolle I 2016 *Handbook of Concentrator Photovoltaic Technology* (Chichester: Wiley) p. 65

[13] Ashcroft N W and Mermin N D 1976 *Solid State Physics* (New York: Cengage Learning) p. 662

[14] Huang H 2010 *Nat. Photon.* **4** 134

[15] Huang F and Liu X 2013 *Appl. Phys. Lett.* **102** 103501

[16] Lopez-Varo P, Bertoluzzi L, Bisquert J, Alexe M, Coll M, Huang J, Jimenez-Tejada J A, Kirchartz T, Nechache R, Rosei F and Yuan Y 2016 *Phys. Rep.* **653** 1

[17] Yang S Y, Seidel J, Byrnes S J, Shafer P, Yang C H, Rossell M D, Yu P, Chu Y H, Scott J F, Ager J W, Martin L W and Ramesh R 2010 *Nat. Nanotechnol.* **5** 143

[18] Yan T L, Chen B, Liu G, Niu R P, Shang J, Gao S, Xue W H, Jin J, Yang J R and Li R W 2017 *Chin. Phys. B* **26** 067702

[19] Wang W, Liu F, Man Lau C, Wang L, Yang G, Zheng D and Li Z 2014 *Appl. Phys. Lett.* **104** 123901

[20] Fathi M, Abderrezek M and Djahli F 2017 *Opt. — Int. J. Light Electron Opt.* **8** 14

[21] Petrova-Koch V, Hezel R and Goetzberger A 2008 *High-Efficient Low-Cost Photovoltaics: Recent Developments*, Vol. 140 (Berlin: Springer) p. 177

[22] Van Sark W G J H M, Barnham K W J, Slooff L H, Chatten A J, Büchtemann A, Meyer A, McCormack S J, Koole R, Farrell D J, Bose R, Bende E E, Burgers A R, Budel T, Quilitz J, Kennedy M, Meyer T, Donegá C D M, Meijerink A and Vanmaekelbergh D 2008 *Opt. Express* **16** 21773

[23] Vossen F M, Aarts M P J and Debije M G 2016 *Energy Build.* **113** 123

[24] Zhang F, Zhang N N, Zhang Y, Yan S, Song S, Jun B and Chen G 2017 *Chin. Phys. B* **26** 054201

[25] Vasiliev M, Alameh K and Nur-E-Alam M 2018 *Appl. Sci.* **8** 849

[26] Richards B S 2006 *Sol. Energy Mater. Sol. Cells* **90** 1189

[27] Brovelli S, Meinardi F and Carulli F (European Patent Office) EP3248225A1 [2018-01-18]

[28] Richards B S 2006 *Sol. Energy Mater. Sol. Cells* **90** 2329

[29] Klingshirn C F, Meyer B K, Waag A, Hoffmann A and Geurts J 2010 *Zinc Oxide*, Vol. 120 (Berlin: Springer) p. 8

[30] Ehrt D 2002 *Comptes Rendus Chim.* **5** 679

[31] Jalili M, Basatani S, Ghahari M and Mohajerani E 2018 *Adv. Powder Technol.* **29** 855

[32] Salem M S, Zekry A, Shaker A and Abouelatta M 2016 2016 *IEEE 43rd Photovoltaic Specialists Conference* (PVSC), June 5–10, 2016, Portland, USA p. 2393

[33] Atlas 2005 *Device Simulator ATLAS User's Manual*

[34] Bucur I C, Tănase L C, Abramiuc L E, Lungu G A, Chirilă C, Trupină L, Apostol N G, Costescu R M, Negrea R F, Pintilie L and Teodorescu C M 2018 *Appl. Surf. Sci.* **432** 27

[35] Kim J H, Li X, Wang L S, de Clercq H L, Fancher C A, Thomas O C and Bowen K H 2001 *J. Phys. Chem. A* **105** 5709

[36] Brendel R and Queisser H 1993 *Sol. Energy Mater. Sol. Cells* **29** 397